

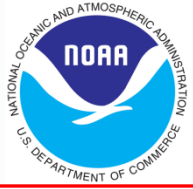
# JPSS STAR Science Team Annual Meeting VIIRS SDR Team

Changyong Cao  
VIIRS SDR Lead  
May 12-16, 2014

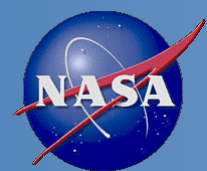




# Outline



- Overview
  - Products, Requirements, Team Members, Users, Accomplishments
- SNPP Algorithms Evaluation:
  - Algorithm Description, Validation Approach and Datasets, Performance vs. Requirements, Risks/Issues/Challenges, Quality Monitoring, Recommendations
- Future Plans
  - Plan for JPSS-1 Algorithm Updates and Validation Strategies, Schedule and Milestones
- Summary



# VIIRS SDR Team



| Leads             | Organization        | Members   |
|-------------------|---------------------|---|
| Changyong Cao     | NOAA/NESDIS/STAR    | Slawomir Blonski, Frank Padula, Wenhui Wang, Jason Choi, Sirish Uprety, Sean Shao, Yan Bai, Vicky Lin                                     |
| Frank Deluccia    | The Aerospace Corp. | David Moyer, Kameron Rausch, others   |
| J. Xiong/R. Wolfe | NASA/VCST           | Hassan Oudrari, Vincent Chang, Aisheng Wu, John Fulbright, Jeff McIntire, Boriana Efrnova, Ning Lei, Gary Lin, Masahiro Nishihama, others |
| Lushalan Liao     | NGAS                | Ronsan Chu, Stephnie Weiss, Tahru Ohnuki, Frank Sun, others   |
| Chris Moeller     | U. Wisc.            | others  |
| Products:         |                     |   |

22 SDRs

Users:

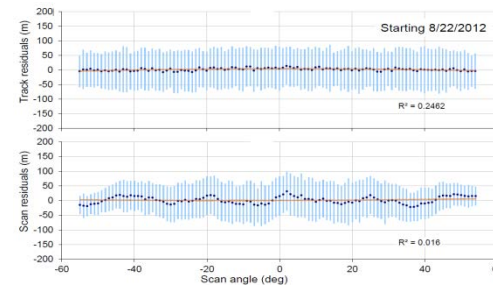
VIIRS EDR with more than 20 products

# Major Achievements

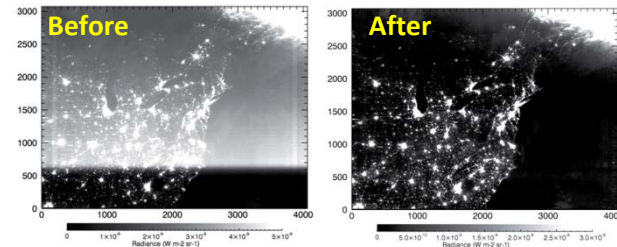
## Major Achievements Since Provisional

- VIIRS on-orbit performance is well characterized & meets specifications
- RSBAutoCal being tested and independently validated by NOAA
- VIIRS DNB Straylight Correction implemented (Aug. 2013); tool kit has been evaluated by NOAA
- Geo-location uncertainties for I-/M-bands are  $\sim 70$  m at nadir, meeting specifications at nadir and edge-of-scan (DNB terrain corrected geo-location product is expected in Mx8.3 in March 2014)

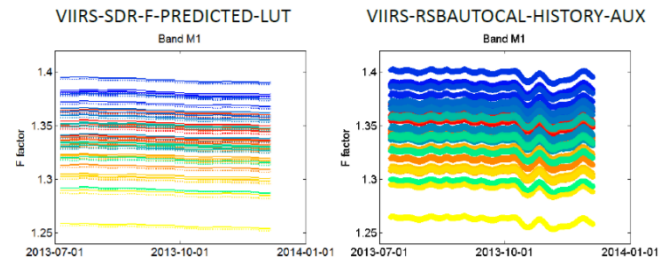
### Geo-Location Accuracy

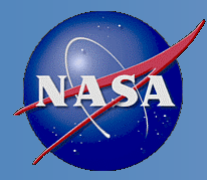


### DNB Straylight Correction Implemented

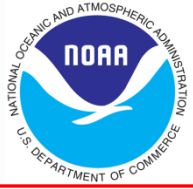


### RSBAutoCal Testing





# Major Achievements and Events

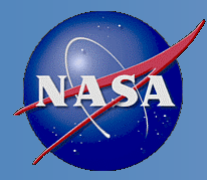


Since the validated maturity workshop in December 2013:

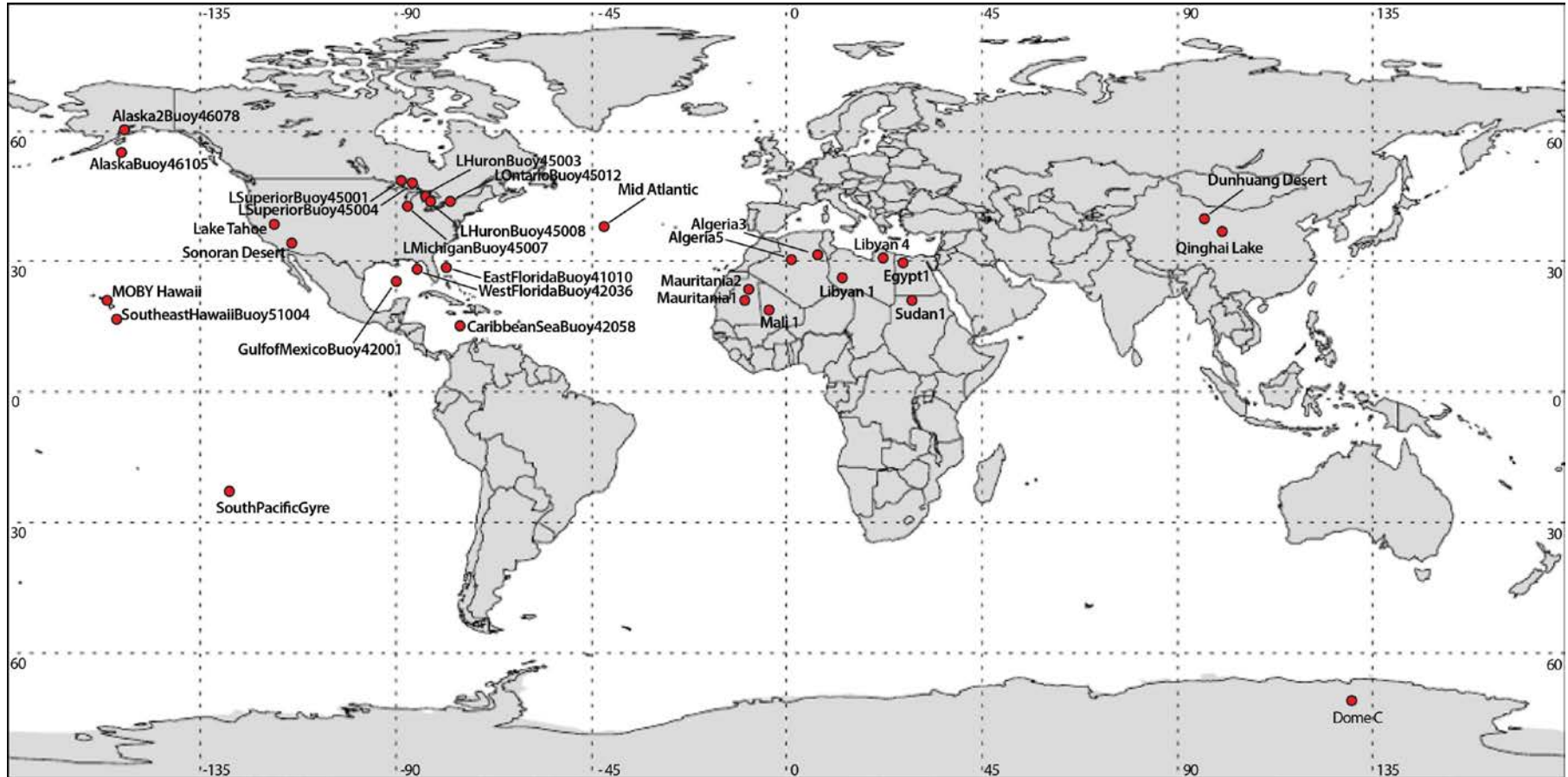
- VIIRS SDR achieved validated maturity
- Validation time series developed for ~30 sites worldwide (W. Wang)
- DCC time series since launch established (W. Wang)
- Lunar band ratio time series developed (S. Shao & J. Choi)
- Calibration coefficient changes ( $c_0=0$ ) implemented (May 2014)
- I3/M10 bias studies (new results from Lunar band ratio analysis, see X. Shao in breakout session)
- Sun vector error findings (NASA)
- DNB terrain corrected geolocation (March 18, 2014 with MX8.4)
- Single Board Computer Lockup(SBC) #6 (or 7), aka “Petulant mode” on Feb. 4, 2014
- Flattening in the degradation shown in H and F factors
- VIIRS J1 polarization studies

On-going work:

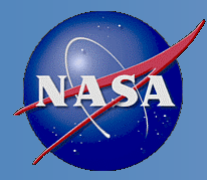
- Continued updating the calibration knowledge base, with new events analyzed and documented
- Continued bias time series analysis between VIIRS and MODIS
- Continued longterm trending and monitoring



# VIIRS Radiometric Validation Time Series at thirty validation sites world-wide

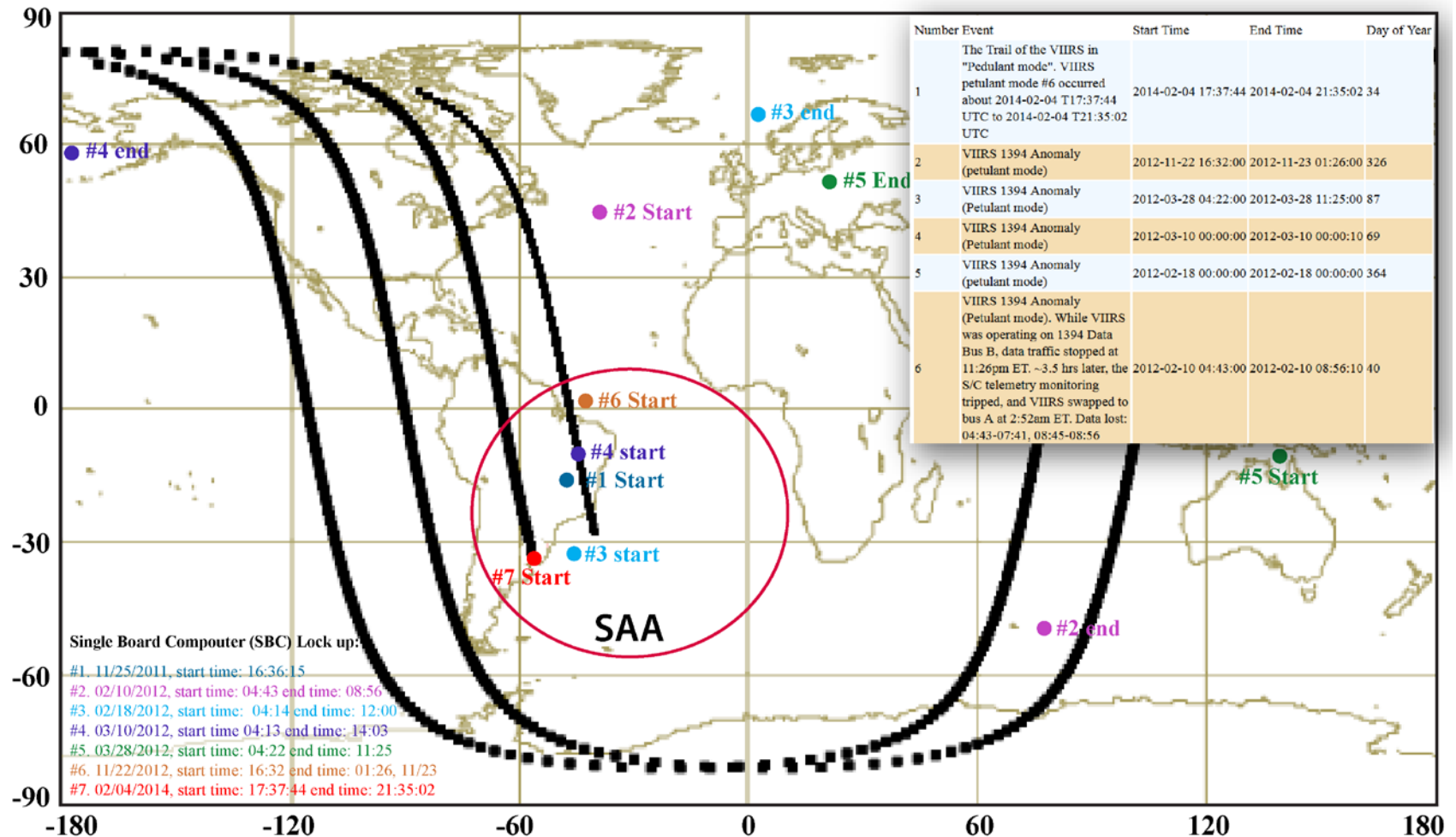


More details will be presented by W. Wang in the VIIRS  
Breakout session



# VIIRS Event Log Database

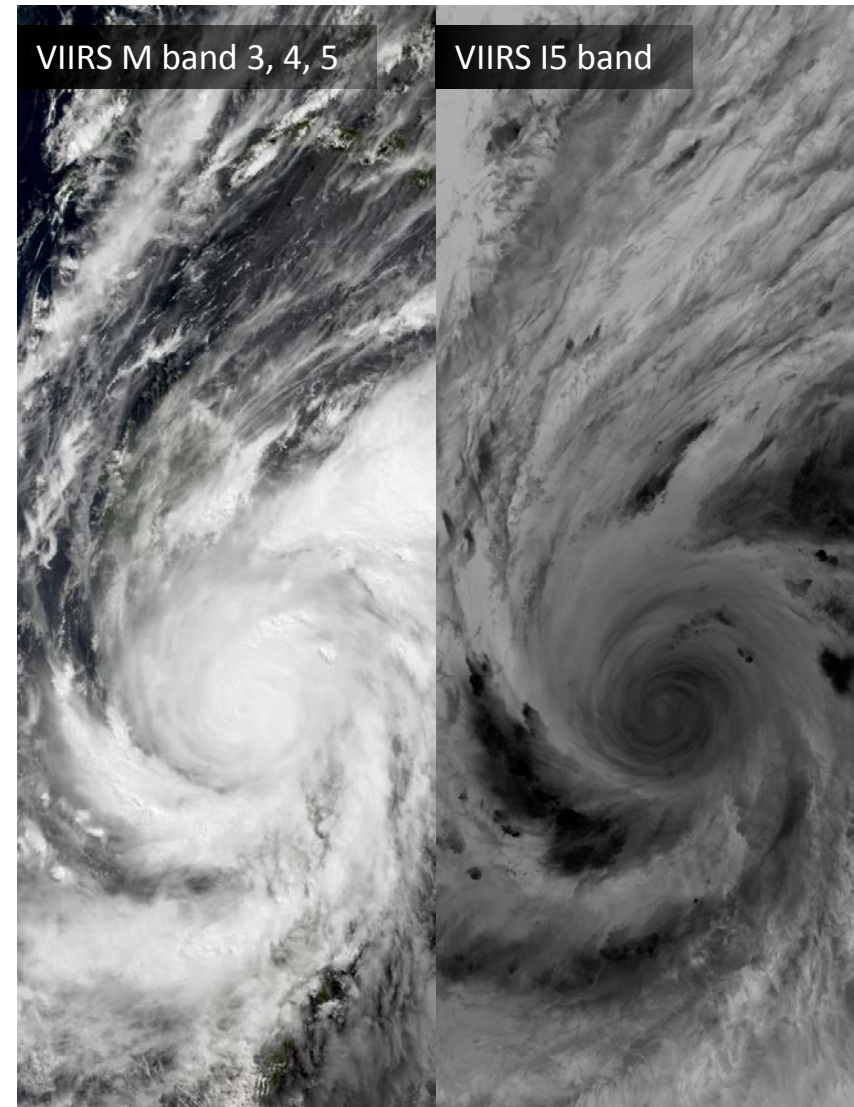
An important part of the Calibration Knowledge base



For more details, see poster by Y. Bai et al.



- **Milestone:** Successfully completed the VIIRS SDR Validated Maturity Workshop, and achieved validated status in March 2014.
- **Accomplishments**
  - STAR held a three-day Suomi NPP SDR Science and Validated Product Maturity Review (December 18-20, 2013) at the NOAA NCWCP to assess the readiness of the VIIRS SDR data product maturity
  - The VIIRS SDR team members and EDR users reported on the progress made since the Provisional Maturity Review demonstrating the VIIRS SDR maturity level
  - Concluding the Workshop the review panel members reached consensus that overall the VIIRS SDR product has reached the validated status and therefore is recommended to be approved by the Algorithm Executive Review Board (AERB)
  - The AERB approved the recommended validated status in March 2014.
- **Significance:** VIIRS SDR has achieved the validated maturity



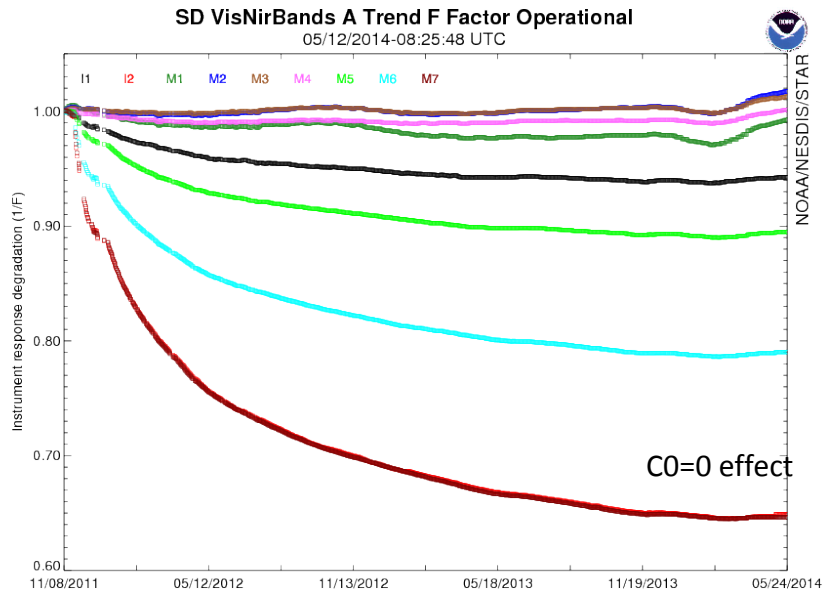




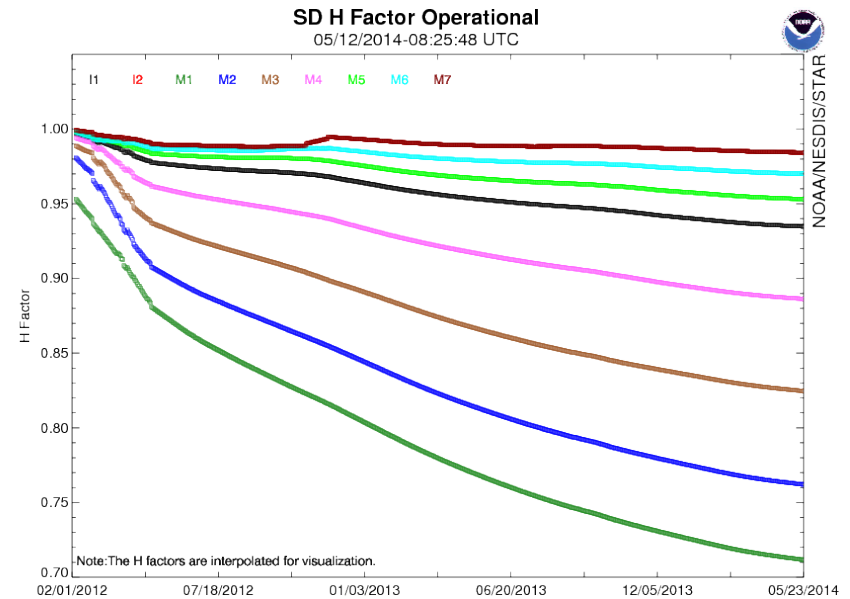
# VIIRS SDR Accuracy



|           | Requirement (absolute uncertainty for uniform scenes)  | Prelaunch and onboard calibration   | Validation: Relative to MODIS/CrIS/IASI/other thru Inter-comparisons  | Note  |
|-----------|--|---|---|---|
| VIIRS RSB | 2% typical reflectance;<br>0.3% stability;<br>0.1% desirable for Ocean Color Applications  | 1.2% for M1-M7;<br>1.5% for M8&9<br>1.4% for M10<br>1.3% for I1&I2<br>1.6% for I3     | 2% ( $\pm 1\%$ ) for matching bands   | Except bands with very low signal (ex. M11); <b>sub-percent accuracy for OC is very challenging.</b><br>Geolocation error: expectation is half I-band pixel; achieved better than quarter I-band pixel ( $1-\sigma$ ) |
| VIIRS TEB | M12/M13: 0.7%(0.13K) @270K<br>M14: 0.6% (0.26K) @ 270K<br>M15/M16: 0.4% (0.22K/0.24K) @270K<br>I4: 5% (0.97K) @270K<br>I5: 2.5% (1.5K) @270K | Better than 0.13K for all M bands except M13 (0.14);<br>0.47K for I4;<br>0.23K for I5 | 0.1K based on statistical comparison with MODIS and CrIS<br>ER-2/SHIS Aircraft underflight shows excellent agreement<br><b>M15 0.4 K bias relative to CrIS at 200K (in spec.)</b> | M15 at 190K requirement is 2.1% radiance or 0.56K<br>Geolocation uncertainty: expectation was half I-band pixel; achieved better than quarter I-band pixel ( $1-\sigma$ )   |
| VIIRS DNB | <ul style="list-style-type: none"> <li>5%, 10%, 30% <math>L_{\min}</math> (LGS, MGS, HGS)</li> </ul>   | 3.5%, 7.8%, and 11% (LGS, MGS, HGS)   | <ul style="list-style-type: none"> <li>4%, 7.7%, 11.8% (LGS, MGS, HGS)</li> </ul>   | Geolocation error is a $\sim 10$ th of a pixel ( $1-\sigma$ ) on the ellipsoid earth but can <b>exceed 1km (up to 24 km at the edges of scan) without terrain correction</b>  |

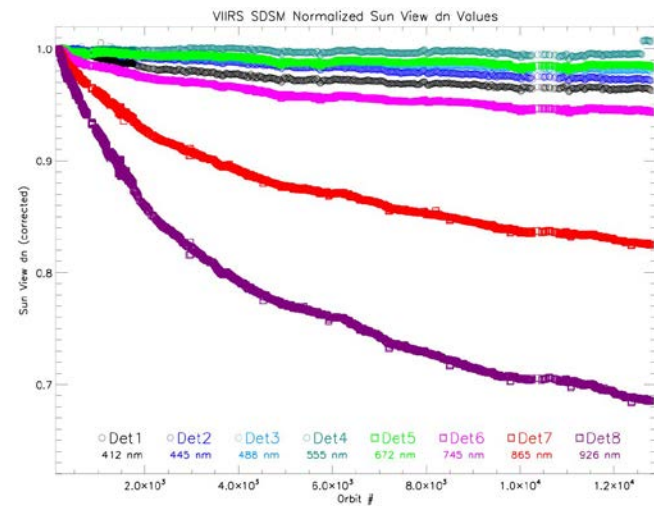
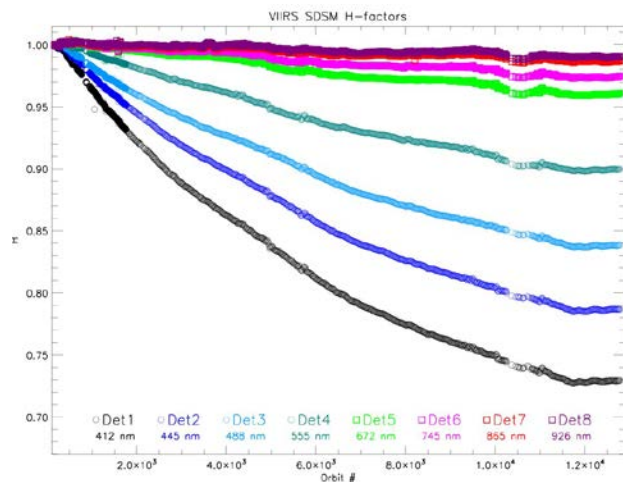
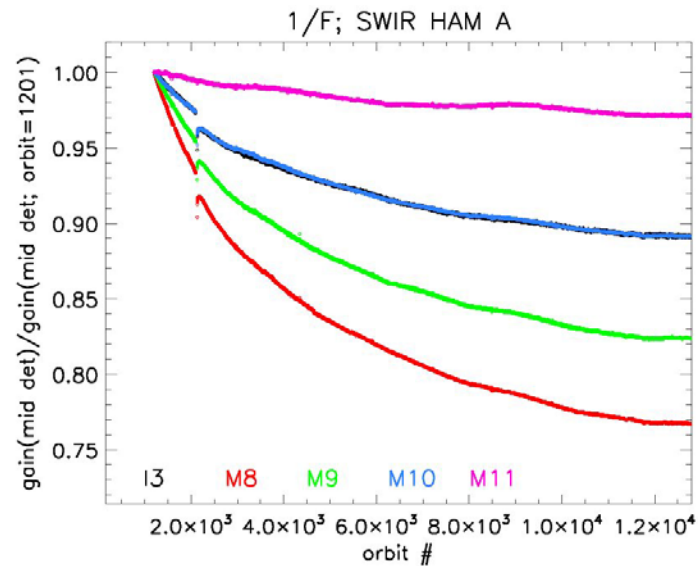
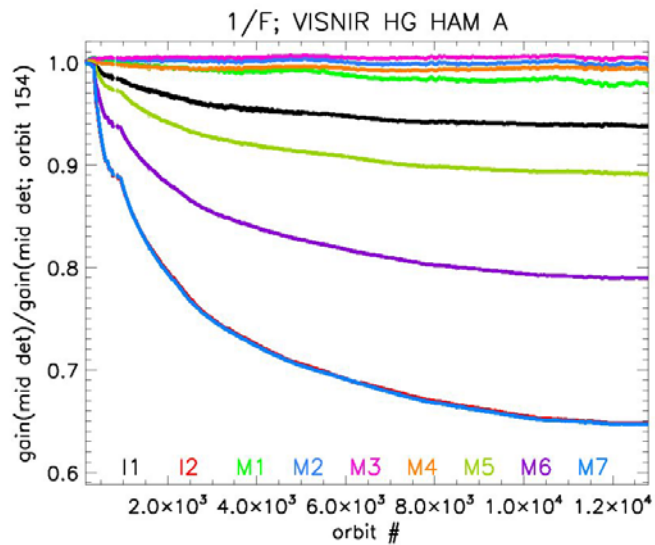


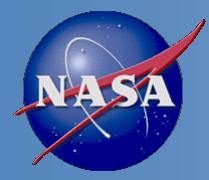
- Recent F-factors show significant trend change which suggests that degradation has stopped or even reversed
- Is this real or artificial?
- How can we tell through validation?
- Is this due to issues in the H-factor calculations?



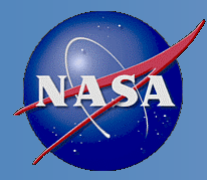
- H-factors in the above plot do not show major recent trend change due to smooth?
- The unsmoothed version does show trend change (such as those produced by Autocal)
- What's the impact on the F-factor calibrations?

What's the impact on EDR products?

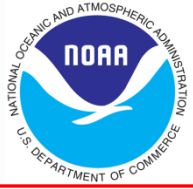




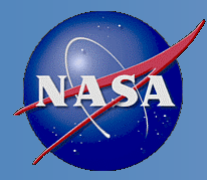
# VIIRS J1 Status Update



# VIIRS J1 Status Update



- Ambient testing: Jan. 2014
- Pre-Environment Review (PER): Feb. 3-6, 2014
- Polarization issue (discussed later)
- Electromagnetic Interference (EMI) testing completed May 2014
  - Sync loss issue resolved for J1
  - Single Board Computer (SBC) Lockup (aka Petulant Mode) issue resolved for J1 (per Gleason and Raytheon)
- Thermal Vacuum testing: Jun.-Oct. 2014

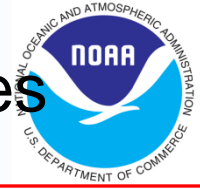
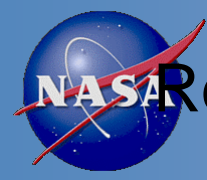


# VIIRS J1 Polarization Studies



- VIIRS J1 polarization sensitivity is significantly out of spec for several bands due to filter coating changes
- The VIIRS SDR team is working closely with the flight and vendor to study mitigation strategies
  - Better characterization through additional prelaunch tests
    - Measure at more scan angles, and T-SIRCUS spectral measurements
  - Better quantification of the polarization phenomenon and VIIRS on-orbit performance
  - Better understanding of impacts on EDR products
- Suomi NPP VIIRS polarization meets the polarization sensitivity specification. VIIRS J2 is expected to meet the specification





# Recent Progress in VIIRS Polarization Related Studies

3/17/2014: Initiated working groups to study the impacts of polarization on products, with several actions from the first telecon on March 17 (M. Goldberg).

4/2/2014: VIIRS SDR special telecon on VIIRS J1 detector level polarization study shows large variation across detectors (presentation by J. McIntire, NASA/VCST)

4/16/2014: MODIS Terra/Aqua prelaunch and on-orbit polarization studies show large increase over the life time of the Terra/MODIS instrument (presentation by J. Xiong, NASA/VCST)

4/24/2014: Recommendations for additional prelaunch testing (telecon ): More measurement angles, monochromatic characterization using T-SIRCUS.

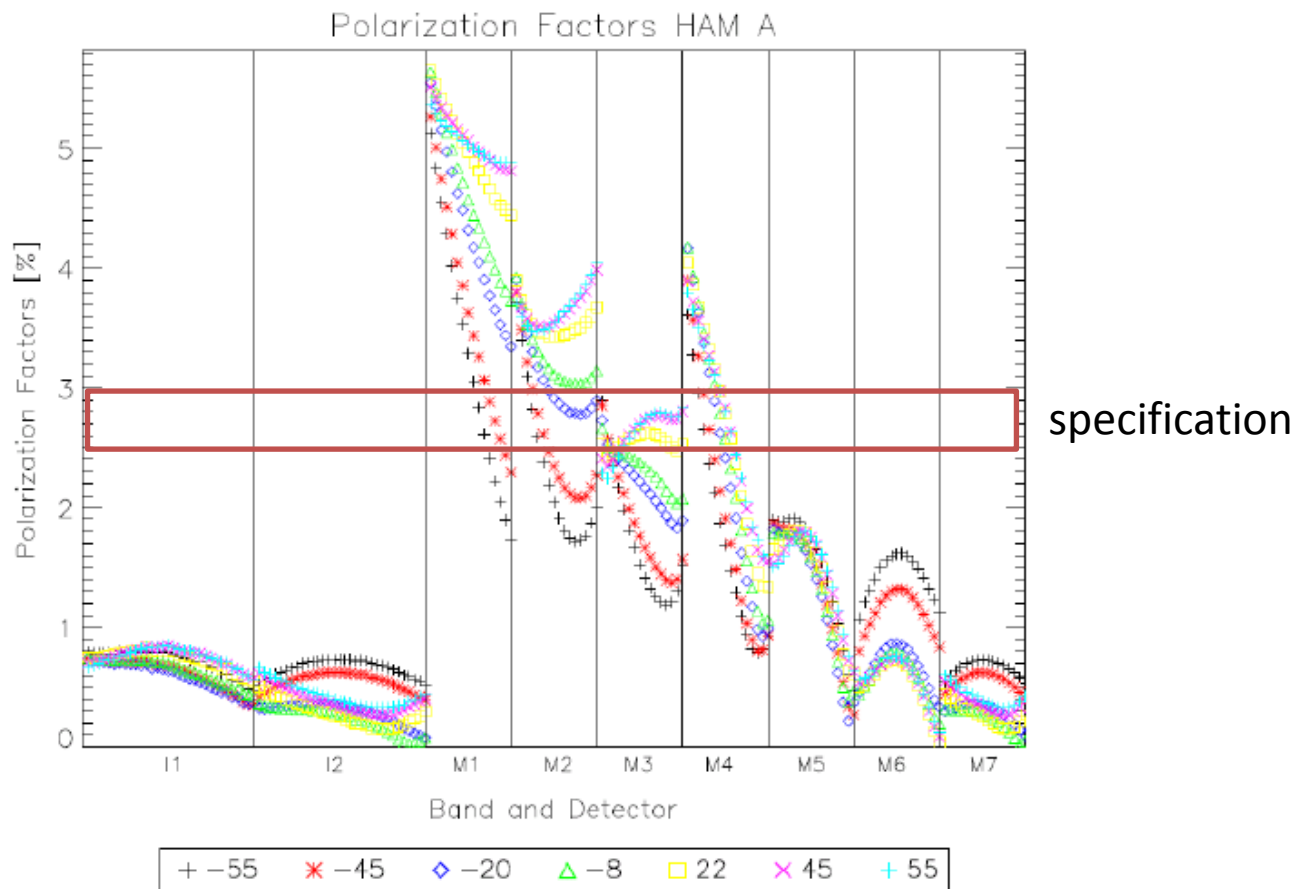
Other progress:

- GOME Polarization Measurement Device (PMD) on MetOp A and B
  - Sample data have been analyzed and a preliminary global map of DoLP map generated.
- Prototype polarization spectroradiometer developed leveraging the ASD spectrometer, with sample in-situ measurements

## Polarization factors (combining all bvonir configurations) – HAM A

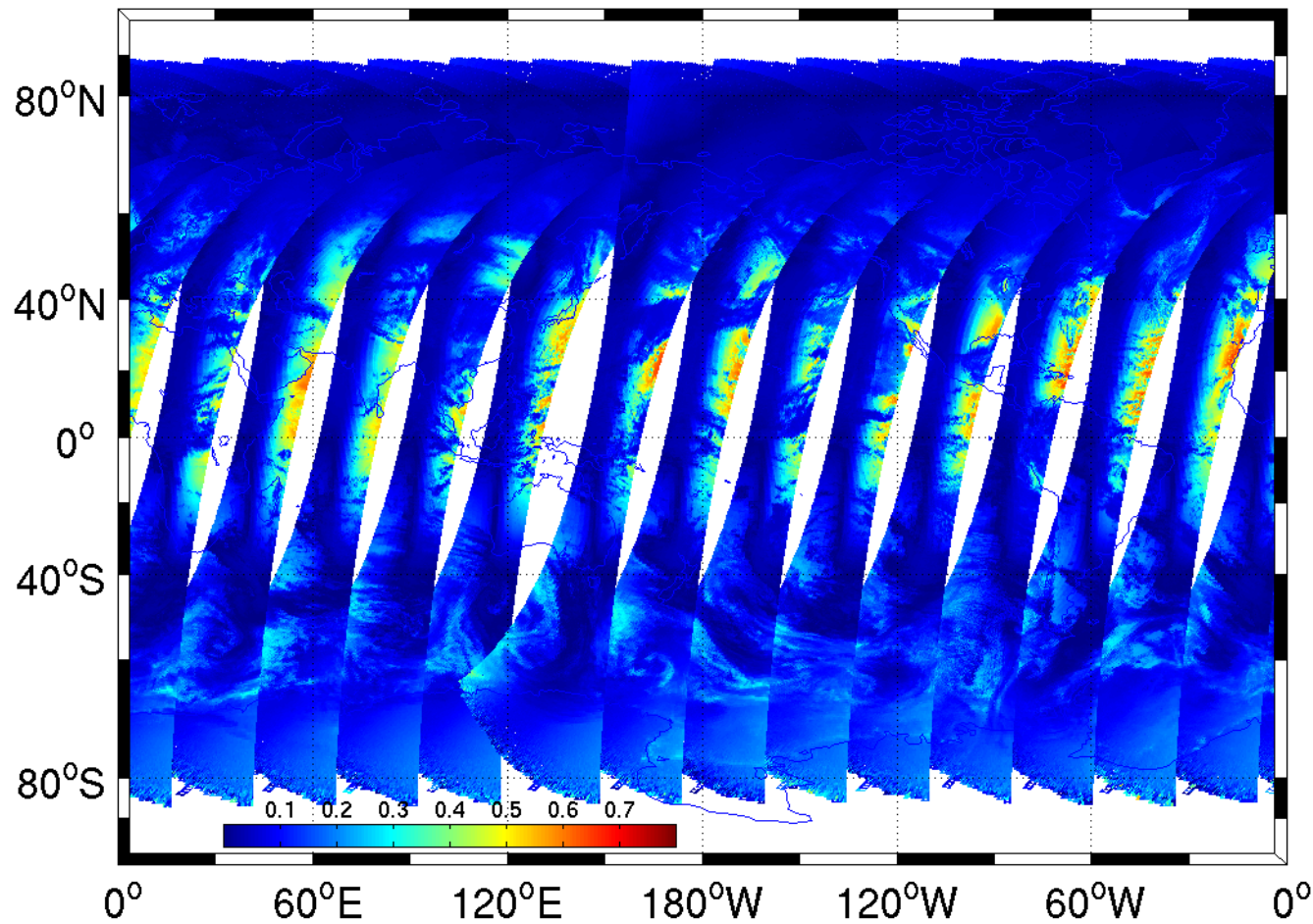
bvonir in: M1-M3; bvonir out: I1-I2, M4-M7

Factors above specification for M1-M4



**DOLP for Wavelength: (PP)413.82 and (PS)413.46**

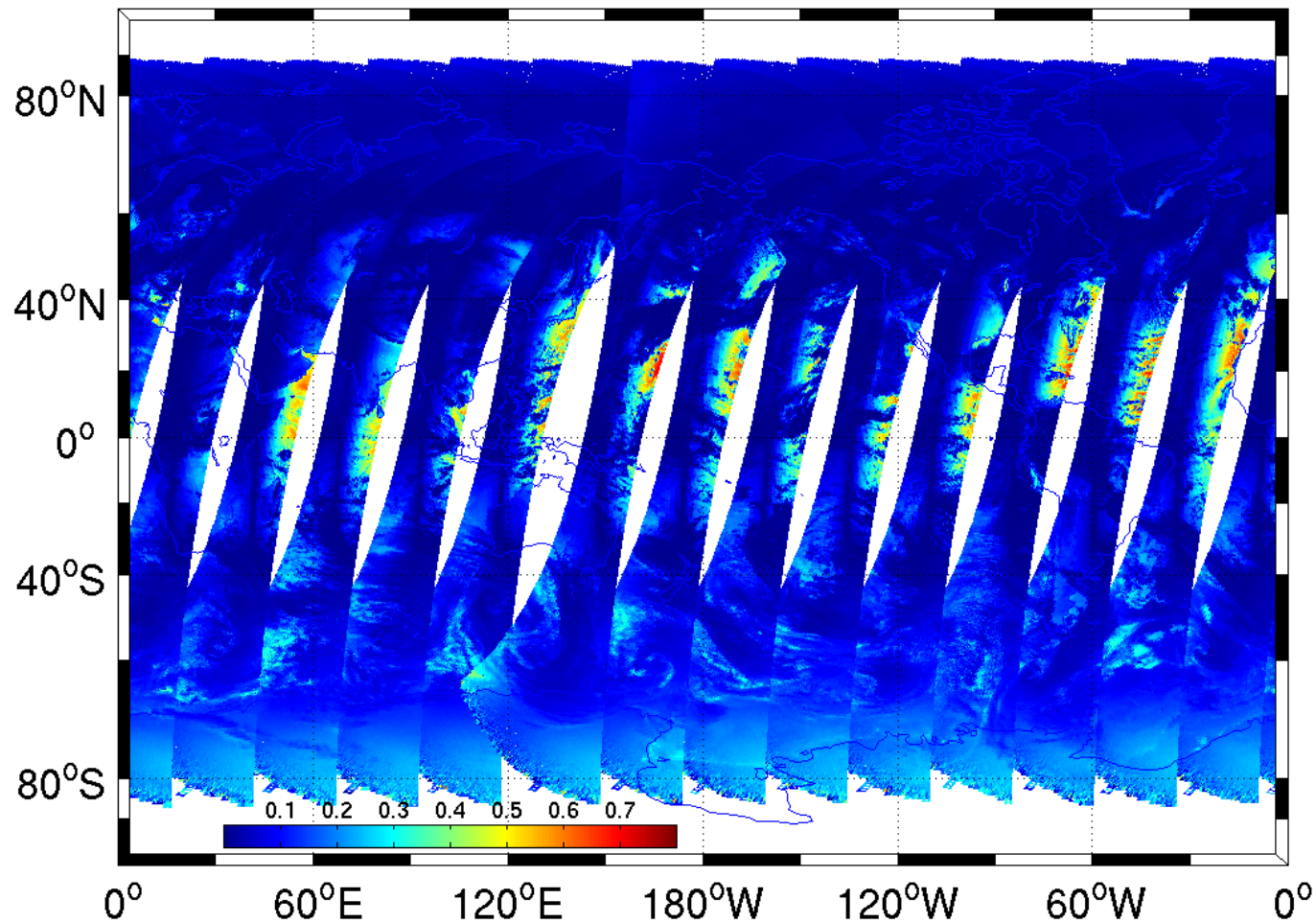
Time: 2014-04-15



preliminary

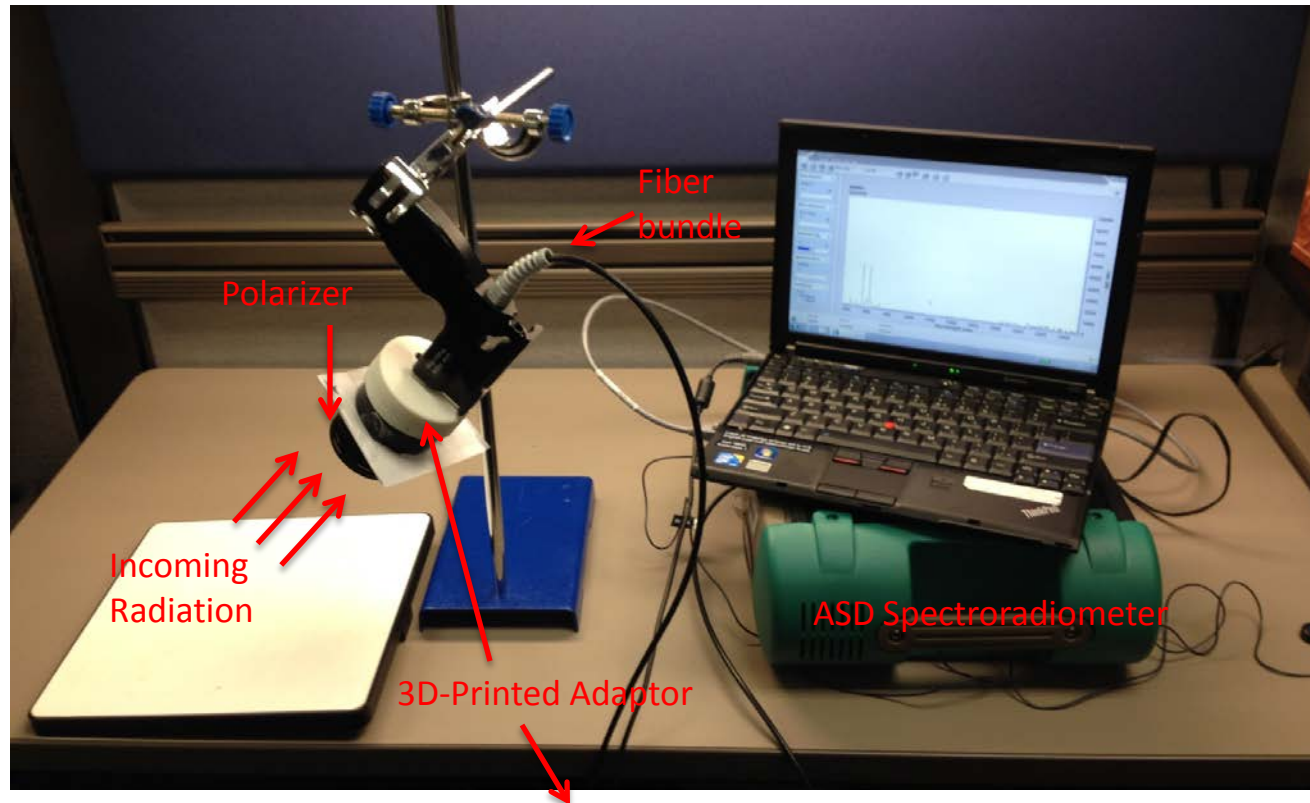
**DOLP for Wavelength: (PP)556.21 and (PS)555.06**

Time: 2014-04-15



preliminary





(Protractor will be replaced with 3D- printed piece)



See poster by A. Pearlman et al for details

# Preliminary Measurement Results

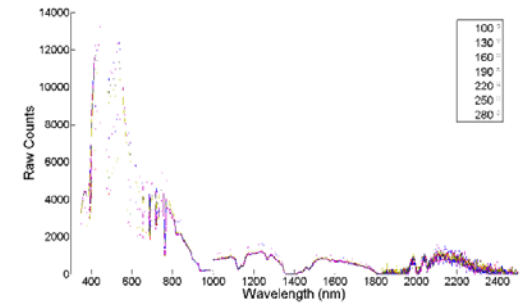
Location: M Square parking lot at 5:38 to 6:00pm (April 17, 2014)

Took measurements of a highly polarized sky:

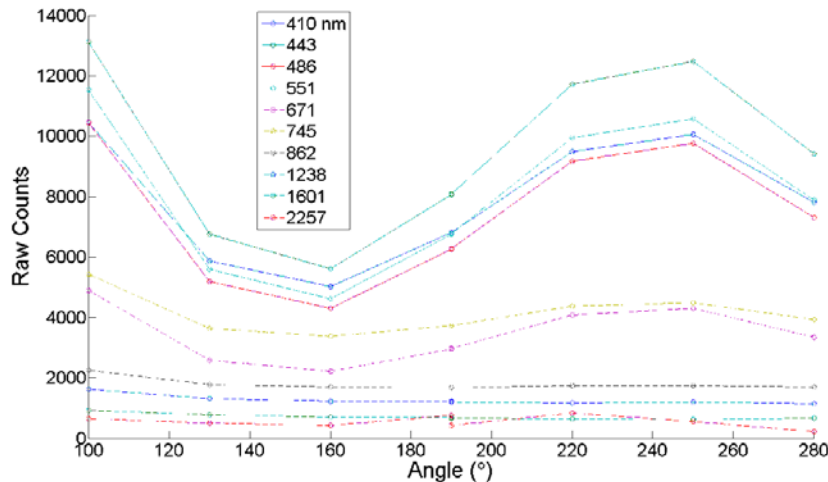
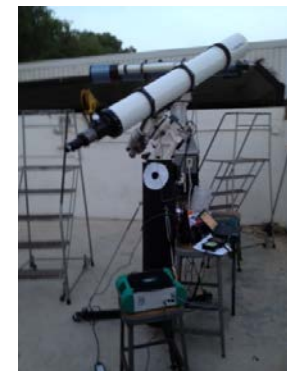
Pointed sensor at  $\sim 90^\circ$  to sun

Mostly clear with cirrus clouds covering  $\sim 75\%$  of sky

Measurement time: 5 minutes



Future plan: Lunar polarization measurements at UMD observatory







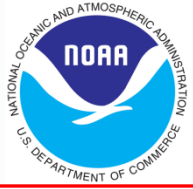
# Issues and Challenges



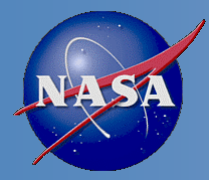
- **Achieving better calibration accuracy for Ocean Color applications**
- **Further improve onboard calibration**
  - RSB autocal, solar vector, etc.
- **Enhance vicarious monitoring capability to ensure high accuracy**
- **Striping in both SST bands and RSB**
- **Detector level RSR performance issues**
- **Polarization effects**
- **Single Board Computer Lockup (SBC), aka “Petulant mode”**
- **Sync loss**
- **J1 VIIRS support**



# Summary

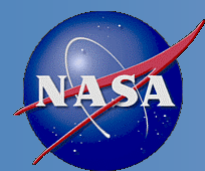


- VIIRS SDR has achieved calibrated/validated Maturity Status in both radiometry and geolocation
- Continue improving the radiometric accuracy to meet Ocean Color application needs
  - Fine tune calibration coefficients (e.g.:  $c_0=0$ )
  - RSB autocal
  - Closely monitoring trend changes
  - Lunar band ratio analysis
- Future work focus on:
  - J1 calibration support, such as polarization studies (observations and RTM)
  - Further enhancements in instrument performance through research (such as striping, detector level processing, improved accuracy, etc)
  - Long term monitoring



# Backup slides





# VIIRS On-orbit Performance Table



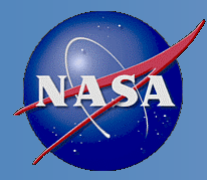
- SDRs = L1b = calibrated, geolocated radiance, reflectance and brightness temperature
- 22 types of SDRs
  - 16 moderate resolution (MOD),
- 11 Reflective Solar Bands (RSB)
- 5 Thermal Emissive Bands (TEB)
  - 5 imaging resolution (IMG),
- 3 RSB; 2 TEB
  - 1 Day Night Band (DNB) imaging, broadband
- 6 non-gridded geolocation products
  - DNB, IMG, IMG terrain corrected, MOD, MOD terrain corrected, MOD unaggregated
- 2 gridded geolocation products
  - MOD, IMG

|                  |          |                     | Specification        |   |               |              |                     |              |                      | Prelaunch                    | On Orbit                     |                              |         |
|------------------|----------|---------------------|----------------------|---|---------------|--------------|---------------------|--------------|----------------------|------------------------------|------------------------------|------------------------------|---------|
|                  | Band No. | Driving EDR(s)      | Spectral Range (um)  | Horiz Sample Interval (km) (track x Scan) |               | Band Gain    | Ltyp or Ttyp (Spec) | Lmax or Tmax | Spec SNR or NEdT (K) | Measured SNR or NEdT (K) (2) | Measured SNR or NEdT (K) (1) | Measured SNR or NEdT (K) (2) |         |
|                  |          |                     |                      | Nadir                                     | End of Scan   |              |                     |              |                      |                              |                              |                              |         |
| Reflective Bands | VisNIR   | M1                  | Ocean Color Aerosol  | 0.402 - 0.422                             | 0.742 - 0.259 | 1.60 x 1.58  | High                | 44.9         | 135                  | 352                          | 616.8                        | 578                          | 588.9   |
|                  |          |                     |                      |   |               |              | Low                 | 155          | 615                  | 316                          | 1092                         | 974                          | 1045.78 |
|                  |          | M2                  | Ocean Color Aerosol  | 0.436 - 0.454                             | 0.742 - 0.259 | 1.60 x 1.58  | High                | 40           | 127                  | 380                          | 622.4                        | 564                          | 572.02  |
|                  |          |                     |                      |   |               |              | Low                 | 146          | 687                  | 409                          | 1118                         | 975                          | 1010.76 |
|                  |          | M3                  | Ocean Color Aerosol  | 0.478 - 0.498                             | 0.742 - 0.259 | 1.60 x 1.58  | High                | 32           | 107                  | 416                          | 690                          | 611                          | 628.46  |
|                  |          |                     |                      |   |               |              | Low                 | 123          | 702                  | 414                          | 1111                         | 1003                         | 988.54  |
|                  |          | M4                  | Ocean Color Aerosol  | 0.545 - 0.565                             | 0.742 - 0.259 | 1.60 x 1.58  | High                | 21           | 78                   | 362                          | 581.1                        | 522                          | 534.96  |
|                  |          |                     |                      |   |               |              | Low                 | 90           | 667                  | 315                          | 963.2                        | 846                          | 856.51  |
|                  |          | I1                  | Imagery EDR          | 0.600 - 0.680                             | 0.371 - 0.387 | 0.80 x 0.789 | Single              | 22           | 718                  | 119                          | 240.7                        | 215                          | 214.07  |
|                  |          | M5                  | Ocean Color Aerosol  | 0.662 - 0.682                             | 0.742 - 0.259 | 1.60 x 1.58  | High                | 10           | 59                   | 242                          | 366.6                        | 321                          | 336.13  |
|                  |          |                     |                      |   |               | Low          | 68                  | 651          | 360                  | 827.9                        | 673                          | 631.26                       |         |
|                  | M6       | Atmosph. Correct.   | 0.739 - 0.754        | 0.742 - 0.776                             | 1.60 x 1.58   | Single       | 9.6                 | 41           | 199                  | 415.2                        | 355                          | 368.4                        |         |
|                  | I2       | NDVI                | 0.846 - 0.885        | 0.371 - 0.387                             | 0.80 x 0.789  | Single       | 25                  | 349          | 150                  | 304.1                        | 251                          | 264.01                       |         |
|                  | M7       | Ocean Color Aerosol | 0.846 - 0.885        | 0.742 - 0.259                             | 1.60 x 1.58   | High         | 6.4                 | 29           | 215                  | 519.8                        | 435                          | 457.54                       |         |
|                  |          |                     |                      |   | Low           | 33.4         | 349                 | 340          | 845.6                | 636                          | 631.24                       |                              |         |
|                  |          |                     |                      |   |               |              |                     |              |                      |                              |                              |                              |         |
| Emissive Bands   | S/WMIR   | M8                  | Cloud Particle Size  | 1.230 - 1.250                             | 0.742 x 0.776 | 1.60 x 1.58  | Single              | 5.4          | 165                  | 74                           | 273                          | 233                          | 221     |
|                  |          | M9                  | Cirrus/Cloud Cover   | 1.371 - 1.386                             | 0.742 x 0.776 | 1.60 x 1.58  | Single              | 6            | 77.1                 | 83                           | 253                          | 231                          | 227     |
|                  |          | I3                  | Binary Snow Map      | 1.580 - 1.640                             | 0.371 x 0.387 | 0.80 x 0.789 | Single              | 7.3          | 72.5                 | 6                            | 172                          | 149                          | 149     |
|                  |          | M10                 | Snow Fraction        | 1.580 - 1.640                             | 0.742 x 0.776 | 1.60 x 1.58  | Single              | 7.3          | 71.2                 | 342                          | 714                          | 550                          | 586     |
|                  |          | M11                 | Clouds               | 2.225 - 2.275                             | 0.742 x 0.776 | 1.60 x 1.58  | Single              | 0.12         | 31.8                 | 10                           | 25                           | 21.8                         | 22      |
|                  |          | I4                  | Imagery Clouds       | 3.550 - 3.930                             | 0.371 x 0.387 | 0.80 x 0.789 | Single              | 270          | 353                  | 2.5                          | 0.4                          | 0.4                          | 0.4     |
|                  |          | M12                 | SST                  | 3.660 - 3.840                             | 0.742 x 0.776 | 1.60 x 1.58  | Single              | 270          | 353                  | 0.396                        | 0.13                         | 0.13                         | 0.13    |
|                  |          | M13                 | SST Fires            | 3.973 - 4.128                             | 0.742 x 0.259 | 1.60 x 1.58  | High                | 300          | 343                  | 0.107                        | 0.04                         | 0.042                        | 0.04    |
|                  |          |                     |                      |   |               |              | Low                 | 380          | 634                  | 0.423                        |                              |                              |         |
|                  |          |                     |                      |   |               |              |                     |              |                      |                              |                              |                              |         |
|                  | LWIR     | M14                 | Cloud Top Properties | 8.400 - 8.700                             | 0.742 x 0.776 | 1.60 x 1.58  | Single              | 270          | 336                  | 0.091                        | 0.06                         | 0.06                         | 0.05    |
|                  |          | M15                 | SST                  | 10.263 - 11.263                           | 0.742 x 0.776 | 1.60 x 1.58  | Single              | 300          | 343                  | 0.07                         | 0.03                         | 0.03                         | 0.03    |
|                  |          | I5                  | Cloud Imagery        | 10.500 - 12.400                           | 0.371 x 0.387 | 0.80 x 0.789 | Single              | 210          | 340                  | 1.5                          | 0.4                          | 0.4                          | 0.4     |
|                  |          | M16                 | SST                  | 11.538 - 12.488                           | 0.742 x 0.776 | 1.60 x 1.58  | Single              | 300          | 340                  | 0.072                        | 0.04                         | 0.03                         | 0.03    |

(1) The Aerospace Corporation (2) NASA NICSE

HSI uses 3 in-scan pixels aggregation at Nadir

Source: VIIRS user's guide. On orbit values (last two columns for March 8, 2012) are updated based on the Murphy table for RSB, provided by Aerospace; TEB values are provided by STAR and NASA.



# VIIRS Sensor Specification

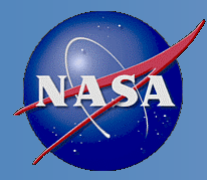
## - RSB sensitivity



**Table: 3.1.5.6.1-1 Sensitivity requirements for VIIRS Sensor reflective bands**

| Band  | Center Wavelength (nm) | Gain Type | Single Gain |     | Dual Gain |     |          |     |
|---|------------------------|-----------|-------------|-----|-----------|-----|----------|-----|
|   |                        |           |             |     | High Gain |     | Low Gain |     |
| .   | .                      | .         | Ltyp        | SNR | Ltyp      | SNR | Ltyp     | SNR |
| M1  | 412                    | Dual      | -           | -   | 44.9      | 352 | 155      | 316 |
| M2  | 445                    | Dual      | -           | -   | 40        | 380 | 146      | 409 |
| M3  | 488                    | Dual      | -           | -   | 32        | 416 | 123      | 414 |
| M4  | 555                    | Dual      | -           | -   | 21        | 362 | 90       | 315 |
| M5  | 672                    | Dual      | -           | -   | 10        | 242 | 68       | 360 |
| M6  | 746                    | Single    | 9.6         | 199 | -         | -   | -        | -   |
| M7  | 865                    | Dual      | -           | -   | 6.4       | 215 | 33.4     | 340 |
| M8  | 1240                   | Single    | 5.4         | 74  | -         | -   | -        | -   |
| M9  | 1378                   | Single    | 6           | 83  | -         | -   | -        | -   |
| M10   | 1610                   | Single    | 7.3         | 342 | -         | -   | -        | -   |
| M11   | 2250                   | Single    | 0.12        | 10  | -         | -   | -        | -   |
| I1  | 640                    | Single    | 22          | 119 | -         | -   | -        | -   |
| I2  | 865                    | Single    | 25          | 150 | -         | -   | -        | -   |
| I3  | 1610                   | Single    | 7.3         | 6   | -         | -   | -        | -   |
| <p>Notes:</p> <p>The units of spectral radiance for Ltyp are <math>\text{watt m}^{-2} \text{sr}^{-1} \mu\text{m}^{-1}</math>.</p> <p>The SNR column shows the minimum required (worst-case) SNR that applies at the end-of-scan. Elsewhere in the scan, aggregation will yield a larger SNR.</p> <p>Within the same gain setting, at radiances larger than Ltyp, the SNR will be larger than what is specified in this table.</p> |                        |           |             |     |           |     |          |     |

**Absolute radiometric calibration uncertainty for uniform scenes: < 2%**



# VIIRS Sensor Specification

## - TEB sensitivity



**Table: 3.1.5.6.2-1 Sensitivity requirements for VIIRS Sensor emissive bands**

| Band | Center Wavelength (nm) | Gain Type | Single Gain |       | Dual Gain |       |          |       |
|------|------------------------|-----------|-------------|-------|-----------|-------|----------|-------|
|      |                        |           |             |       | High Gain |       | Low Gain |       |
| .    | .                      | .         | Ttyp        | NEdT  | Ttyp      | NEdT  | Ttyp     | NEdT  |
| M12  | 3700                   | Single    | 270         | 0.396 | -         | -     | -        | -     |
| M13  | 4050                   | Dual      | -           | -     | 300       | 0.107 | 380      | 0.423 |
| M14  | 8550                   | Single    | 270         | 0.091 | -         | -     | -        | -     |
| M15  | 10763                  | Single    | 300         | 0.070 | -         | -     | -        | -     |
| M16  | 12013                  | Single    | 300         | 0.072 | -         | -     | -        | -     |
| I4   | 3740                   | Single    | 270         | 2.500 | -         | -     | -        | -     |
| I5   | 11450                  | Single    | 210         | 1.500 | -         | -     | -        | -     |

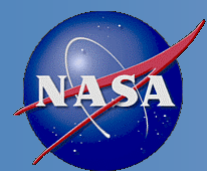
**Notes:**

The NEdT column corresponds to the minimum required (worst-case) SNR that applies at the end-of-scan. Elsewhere in the scan, aggregation will yield a larger SNR.

Within the same gain setting, at scene temperatures larger than Ttyp, the SNR will be larger than at Ttyp.

For reference, the NEdT values in Table 15 are related to the noise equivalent spectral radiance (NEdL) by the following formula:





# VIIRS Sensor Specification

## - TEB Uncertainty

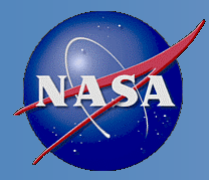


**Table: 3.1.5.9.2.3-1 Absolute radiometric calibration uncertainty of spectral radiance for moderate resolution emissive bands**

| Band | $\lambda_c$ ( $\mu\text{m}$ ) | Scene Temperature |      |      |      |      |
|------|-------------------------------|-------------------|------|------|------|------|
|      |                               | 190K              | 230K | 270K | 310K | 340K |
| M12  | 3.7                           | N/A               | 7.0% | 0.7% | 0.7% | 0.7% |
| M13  | 4.05                          | N/A               | 5.7% | 0.7% | 0.7% | 0.7% |
| M14  | 8.55                          | 12.3%             | 2.4% | 0.6% | 0.4% | 0.5% |
| M15  | 10.763                        | 2.1%              | 0.6% | 0.4% | 0.4% | 0.4% |
| M16  | 12.013                        | 1.6%              | 0.6% | 0.4% | 0.4% | 0.4% |

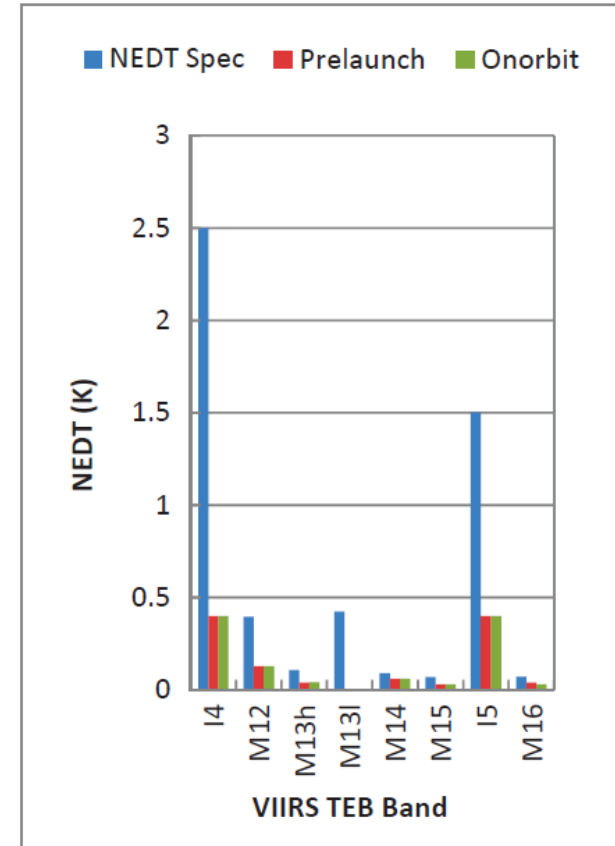
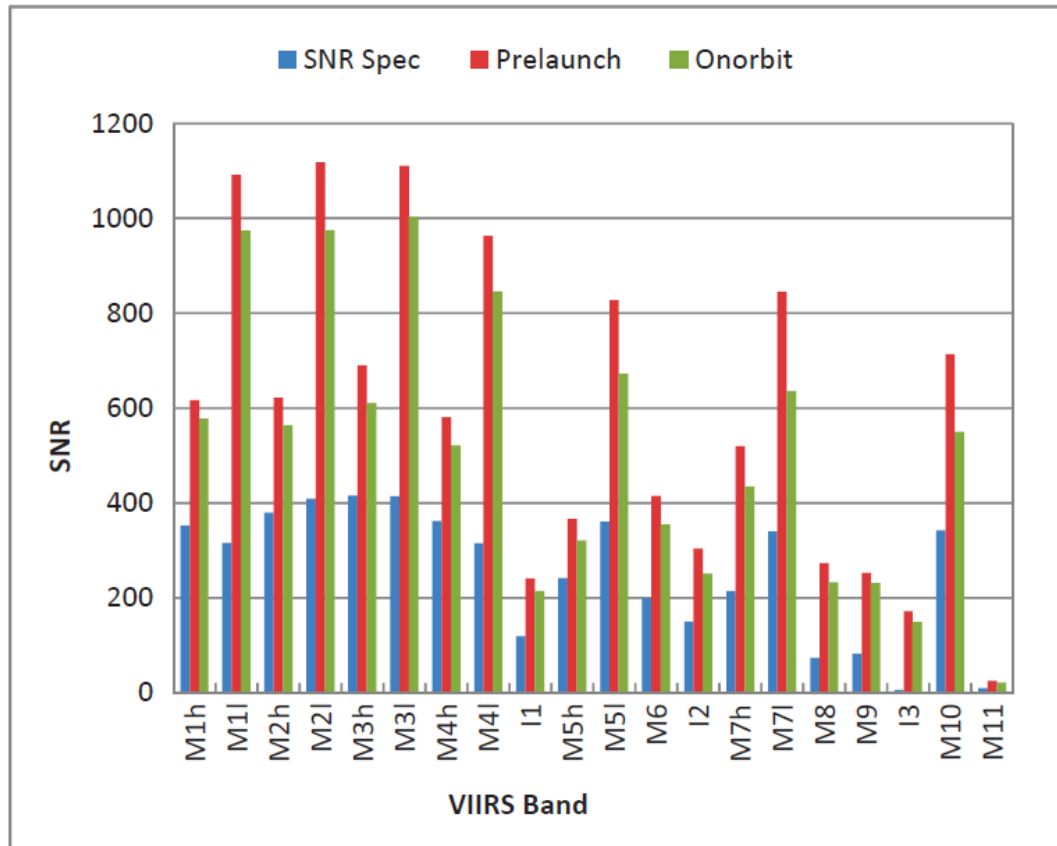
**Table: 3.1.5.9.2.4-1 Radiometric calibration uncertainty for imaging emissive bands**

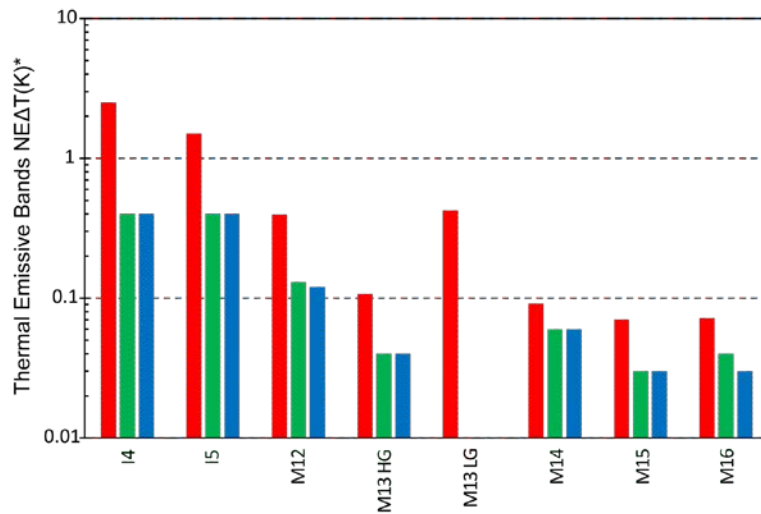
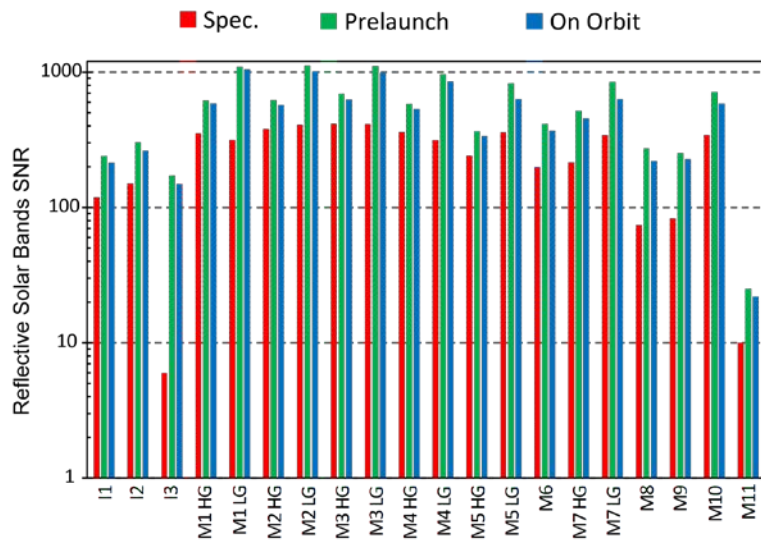
| Band | Center Wavelength (nm) | Calibration Uncertainty |
|------|------------------------|-------------------------|
| I4   | 3740                   | 5.0%                    |
| I5   | 11450                  | 2.5%                    |



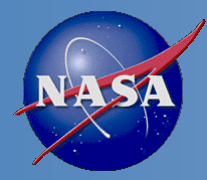
# VIIRS On-orbit Performance

## -SNR and NEDT





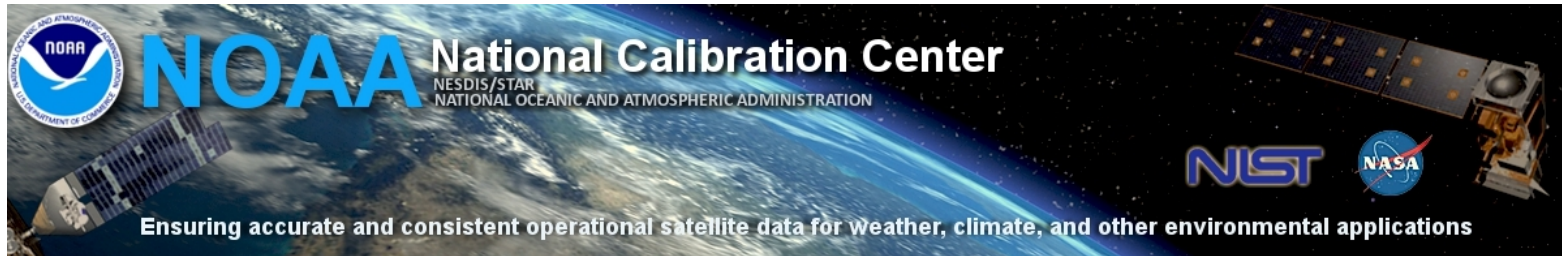
\*Note NE $\Delta$ T(K) is at specific temperatures (see Table 2).



# VIIRS Calibration Knowledge Base Updated



One stop shop for VIIRS SDR information



NCC

You are here: Foswiki > NCC Web > VIIRS (21 Nov 2013, ChangyongCao)

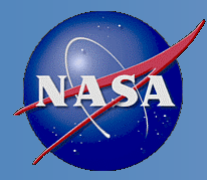
## Visible Infrared Imaging Radiometer Suite (VIIRS)

The Visible Infrared Imaging Radiometer Suite (VIIRS) is one of the key instruments onboard the Suomi National Polar-Orbiting Partnership (Suomi NPP) spacecraft, which was opened on November 21, 2011, which enables a new generation of operational moderate resolution-imaging capabilities following the legacy of the AVHRR on NOAA an operational environmental monitoring and numerical weather forecasting, with 22 imaging and radiometric bands covering wavelengths from 0.41 to 12.5 microns, providing tl records including clouds, sea surface temperature, ocean color, polar wind, vegetation fraction, aerosol, fire, snow and ice, vegetation, , and other applications. Results from calibration and validation have shown that VIIRS is performing very well. **VIIRS paper:** Cao, C., F. DeLuccia, X. Xiong, R. Wolfe, F. Weng, Early On-orbit Performance of the

- Home
- Terms of Reference
- Publication Database
- About
- GOES-R
- NPP/JPSS/VIIRS
- NPP/JPSS/OMPS
- NOAA/AVHRR
- NOAA/SSU
- MetOp
- JASON
- DSCOVR
- Space Weather
- Standards
- Lunar Calibration
- Calibration Sites

| News and Documents                       | VIIRS Performance and Monitoring                        | Data and Software   |
|--|---|---|
| <a href="#">News</a>                     | <a href="#">VIIRS Longterm Monitoring</a>               | <a href="#">VIIRS Image Gallery</a>                           |
| <a href="#">Publication Database</a>     | <a href="#">VIIRS On-orbit Performance Table</a>        | <a href="#">VIIRS data on CLASS</a>                           |
| <a href="#">VIIRS Users Guide</a>        | <a href="#">Standardized Calibration Parameters</a>     | <a href="#">VIIRS data on ftp site (90 days)</a>              |
| <a href="#">VIIRS Calibration ATBD</a>   | <a href="#">VIIRS Spectral Response Functions</a>       | <a href="#">Data on GRAVITE</a>                               |
| <a href="#">Conference Presentations</a> | <a href="#">VIIRS Event Log Database (experimental)</a> | <a href="#">VIIRS Software Tools</a>                          |
| <a href="#">VIIRS Novel Applications</a> | <a href="#">NPP/AQUA SNO Predictions</a>                | <a href="#">Planck Calculator for Infrared Remote Sensing</a> |
| <a href="#">VIIRS SDR Data Format</a>    | <a href="#">Radiometric Intercomparison with MODIS</a>  | <a href="#">VIIRS Line Spread Function along scan</a>         |
| <a href="#">VIIRS SDR Meetings</a>       | <a href="#">VIIRS at Cal/Val Sites</a>                  | <a href="#">VIIRS Cloud Mask (VCM)</a>                        |
| <a href="#">VIIRS FAQ</a>                | <a href="#">Lunar Calendar for DNB</a>                  | <a href="#">SDR/EDR Team</a>                                  |
| <a href="#">About VIIRS</a>              | <a href="#">Moon in Space View Events</a>               | <a href="#">Standard Radiometric Test Scenes</a>              |

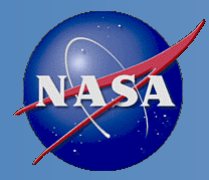
Google "NOAA NCC"



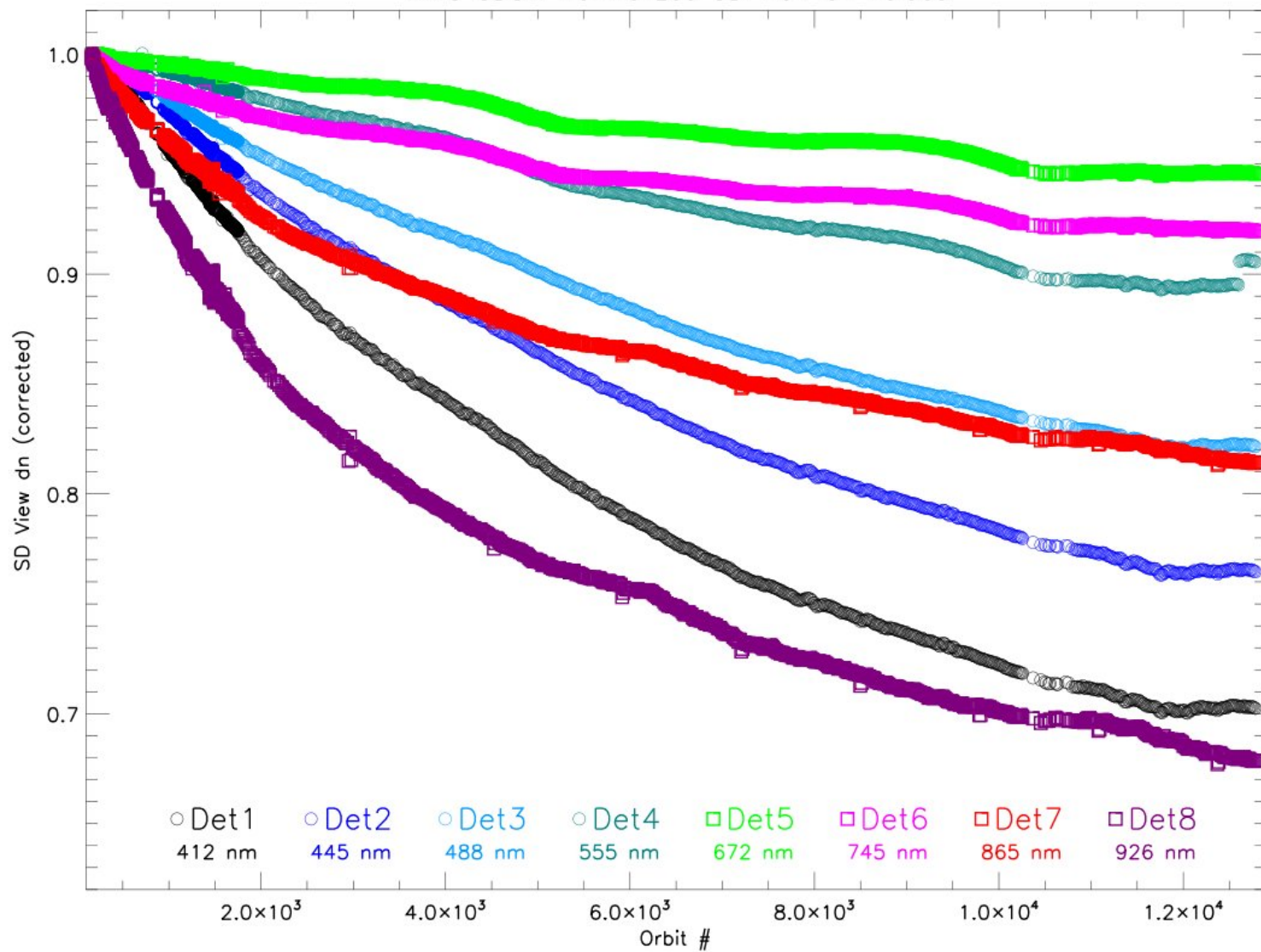
# VIIRS SDR Peer Reviewed Publications



- Cao, C., F. Deluccia, X. Xiong, R. Wolfe, and F. Weng, 2013a, Early On-orbit Performance of the Visible Infrared Imaging Radiometer Suite (VIIRS) onboard the Suomi National Polar-orbiting Partnership (Suomi-NPP) Satellite, IEEE Transaction on Geoscience and Remote Sensing, DOI:10.1109/TGRS.2013.2247768, in press (available online at IEEEXplore).
- Cao, C., X. Xiong, S. Blonski, Q. Liu, S. Uprety, X. Shao, Y. Bai, F. Weng, 2013, Suomi NPP VIIRS sensor data record verification, validation, and long-term performance monitoring, Journal of Geophysical Research: Atmospheres, DOI: 10.1002/2013JD020418
- Cao, C., X. Shao, S. Uprety, (2013b), Detecting Light Outages After Severe Storms Using the Suomi-NPP/VIIRS Day Night Band Radiances, IEEE Geoscience and Remote Sensing Letters, DOI: 10.1109/LGRS.2013.2262258, in press.
- Liu, Q., C. Cao, and F. Weng, 2013, Assessment of Suomi National Polar-Orbiting Partnership VIIRS Emissive Band Calibration and Inter-Sensor Comparisons, IEEE JSTAR, 10.1109/JSTARS.2013.2263197.
- Liao, L.B., S. Weiss, S. Mills, B. Hauss (2013), Suomi NPP VIIRS Day-Night-Band (DNB) On-Orbit Performance, Journal of Geophysical Research-Atmosphere, DOI: 10.1002/2013JD020475
- Wolfe, R., G. Lin, M. Nishihama, K. P. Tewari, J. C. Tilton, A. R. Isaacman et al., 2013, Suomi NPP VIIRS prelaunch and on-orbit geometric calibration and characterization, DOI: 10.1002/jgrd.50873, JGR special issue , in press.
- Rausch, K. et al., VIIRS RSB Autocal, JGR special issue , in press.
- Xiong, X., J. Butler, K. Chiang, B. Efremova, J. Fulbright, N. Lei, J. McIntire, H. Oudrari, J. Sun, Z. Wang, A. Wu (2013), VIIRS On-orbit Calibration Methodology and Performance, Journal of Geophysical Research-Atmosphere, DOI: 10.1002/2013JD020423.
- Uprety, S., C. Cao, X. Xiong, S. Blonski, A. Wu, and X. Shao, 2013, Radiometric Inter-comparison between Suomi NPP VIIRS and Aqua MODIS Reflective Solar Bands using Simultaneous Nadir Overpass in the Low Latitudes, JTech , doi: <http://dx.doi.org/10.1175/JTECH-D-13-00071.1>.



VIIRS SDSM Normalized SD View dn Values



Courtesy of N. Lei, VCST





# Algorithm Evaluations



- In the case of IDPS algorithms, we want the algorithm leads to provide 1 of 3 recommendations:
  1. NPOESS algorithm has evolved into the NOAA-endorsed JPSS algorithm and any needed improvements should continue.
  2. NPOESS (or evolved) algorithm will not meet requirements or effort is too large, replace with NOAA-endorsed JPSS algorithm
  3. NOAA-endorsed algorithm should be used even if NPOESS (or evolved) algorithm meets performance because of legacy, enterprise, blended products, and other considerations.
- For 2 or 3, present the alternative algorithm methodology description, algorithm performance against the level 2 supplement specification and any user assessments.